Molecular Crystals and Liquid Crystals

ISSN: 1542-1406 (Print) 1563-5287 (Online) Journal homepage: http://www.tandfonline.com/loi/gmcl20

Resistor-transistor logic circuits using vertical-type organic transistors

T. Agatsuma, H. Muto & K. Nakayama

To cite this article: T. Agatsuma, H. Muto & K. Nakayama (2016) Resistor-transistor logic circuits using vertical-type organic transistors, Molecular Crystals and Liquid Crystals, 629:1, 187-192, DOI: 10.1080/15421406.2015.1094851

To link to this article: http://dx.doi.org/10.1080/15421406.2015.1094851

Published online: 16 Jun 2016.

MOLECULAR CRYSTALS AND LIQUID CRYSTALS
2016, VOL. 629, 187–192
http://dx.doi.org/10.1080/15421406.2015.1094851

Taylor & Francis
Taylor & Francis Group

Resistor-transistor logic circuits using vertical-type organic transistors

T. Agatsuma[a], H. Muto[a], and K. Nakayama[a,b]

[a]Department of Organic Device Engineering, Graduate School of Science and Engineering, Yamagata University, Jonan, Yonezawa, Yamagata Japan; [b]Research Center for Organic Electronics, Yamagata University, Jonan, Yonezawa, Yamagata Japan

ABSTRACT

NOR gate operation using organic devices was demonstrated based on resistor-transistor logic (RTL). The RTL was composed of an OR gate using two single layered devices as input resistors and a NOT gate (inverter) using a vertical-type metal base organic transistor (MBOT). The input resistors were connected to the base electrode of the MBOT. When either input was turned from low to high voltage, the output voltage changed from high to low, indicating NOR operation. Dynamic characteristics of the RTL circuit was also evaluated, and operation frequency was estimated to be 300 Hz.

KEYWORDS

Metal-base organic transistor; Resistor-transistor logic; NOR gate

Introduction

Organic thin-film transistors have been studied extensively due to the advantages of low temperature fabrication, low production cost, and flexibility [1–3]. In recent years, organic integrated circuits using fully solution-processed organic transistors have been reported [4–6]. These applications are generally based on digital circuits using organic field-effect transistors (OFETs) having a lateral channel. To achieve high operation speed in OFETs, the channel length should be reduced by using a special fine patterning technique. Another approach to reduce the channel length is vertical-type organic transistors. Thus far, several types of vertical-type transistors have been reported [7–12]. In these devices, channel length can be easily reduced to less than 1 μm because it corresponds to thickness of the organic layer; thus, these devices have great potential for high cutoff frequency.

Our proposed metal-base organic transistor (MBOT) [13–15] is high-performance vertical-type organic transistor with a simple layered structure, achieving large output current modulation at low operation voltage. Another notable feature of the MBOT is current amplification behavior similar to a silicon bipolar junction transistor (BJT). BJT is nowadays mainly used for analog circuits; for example, amplifier, filter, and oscillators. However, there exists digital circuits using BJT; for example, resistor transistor logic (RTL), diode transistor logic (DTL), transistor transistor logic (TTL), and so on. These digital circuits had been used before remarkable developments of complementary metal-oxide-semiconductor circuits. To our best

CONTACT K. Nakayama nakayama@yz.yamagata-u.ac.jp 4-3-16 Jonan, Yonezawa, Yamagata 992-8510, Japan
Color versions of one or more of the figures in the article can be found online at www.tandfonline.com/gmcl.
This paper was originally submitted to *Molecular Crystals and Liquid Crystals,* Volumes 620–622, Proceedings of the KJF International Conference on Organic Materials for Electronics and Photonics 2014.

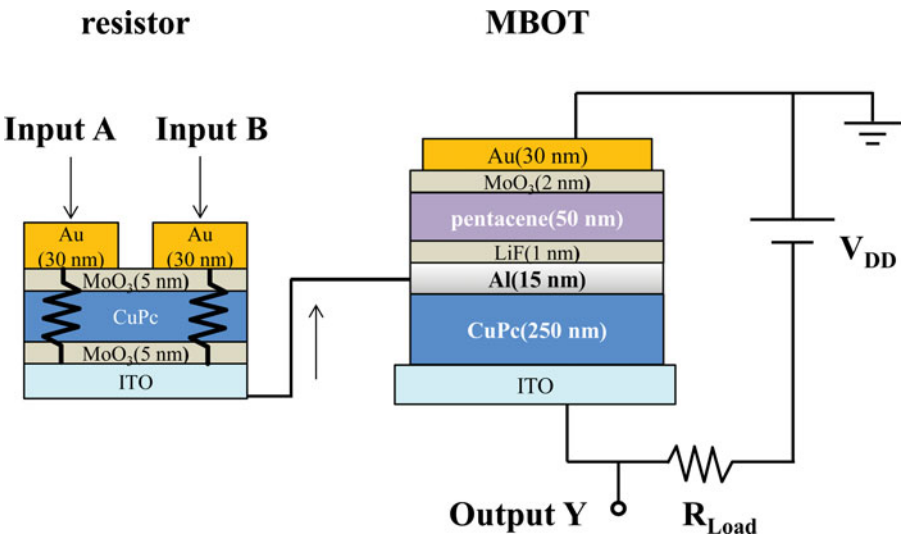

Figure 1. The circuit scheme of the NOR gate based on RTL. The device structure of each component (resistor device and MBOT) is also shown.

knowledge, BJT-based digital circuits using organic transistors have not been reported. In this study, we fabricated a NOR gate based on a resistor-transistor logic using an MBOT instead of silicon BJT. NOR logic has functional completeness, which means that all logic operation can be realized by combination of NOR gates. The NOR gate is composed of an OR gate and a NOT gate. The OR gate was simply fabricated by two single-layered devices as input resistors, and the NOT gate (inverter) was fabricated by an MBOT. The static and dynamic modulation characteristics of the NOR gate was measured.

Experiment

The device structures and circuit scheme for the RTL gate are shown in Fig. 1. A p-type MBOT and two single-layered devices for resistors were separately fabricated by vacuum deposition on each indium tin oxide (ITO) glass substrate. For the p-type MBOT, copper phthalocyanine (CuPc) with a thickness of 250 nm was prepared on a cleaned ITO glass substrate as a collector layer. After deposition of Al (15 nm), the substrate was subjected to heat treatment for one hour at 150°C under atmospheric condition. After deposition of a thin LiF layer (1 nm), an emitter layer of pentacene (50 nm) and a top MoO_3 (2 nm)/Au (30 nm) electrode were evaporated. The ITO electrode, Al/LiF layers, and MoO_3/Au layers were the collector electrode, base electrode, and emitter electrode, respectively. The resistor device included two sets of a single-layered device for input A and B with device structure of MoO_3 (5 nm)/CuPc (250 nm)/MoO_3 (2 nm)/Au (30 nm). The active area of both devices was 0.04 cm^2. The RTL circuit was composed by connecting two resistors to the base electrode of MBOT in parallel.

Current-voltage characteristics of each device were measured by a semiconductor parameter analyzer (Agilent, 4155C) in a N_2-filled glove box. For the MBOT a collector voltage (V_C) was applied between the collector and emitter electrodes, and a base voltage (V_B) was applied between the emitter and base electrodes; in both cases, the emitter was positively biased. For the resistor device two-terminal *J-V* curves was measured. The RTL circuit was evaluated by measuring the output signal voltage (Y) for various combinations of two input signals A and

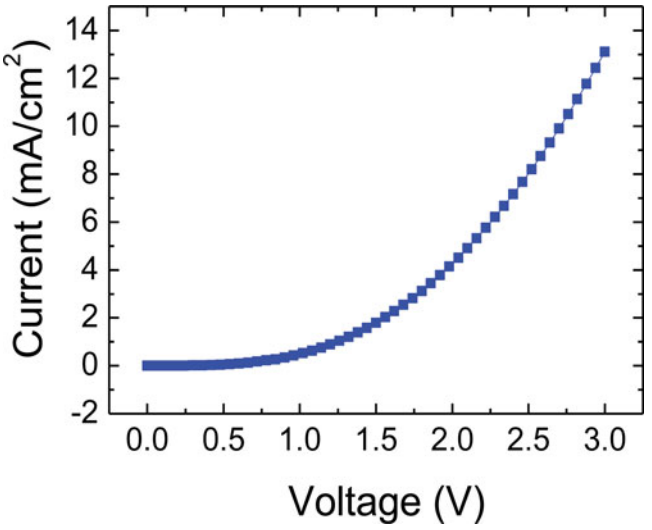

Figure 2. The *J-V* characteristics of the resistor device.

B. Dynamic characteristics of the RTL circuits were measured by using a frequency response analyzer (NF, FRA5096).

Results and discussion

First, electrical characteristics of each component (resistor and MBOT) were evaluated individually. Figure 2 shows the *J-V* characteristics of the resistor device. Although MoO_3 layer was inserted to reduce energy barrier at the organic semiconductor/electrode interface, the *J-V* curve showed nonlinearity. Therefore, the resistance depended on the measured voltage; 5.3×10^6 Ω and 5.7×10^3 Ω at input voltage 0.06 V and 3.0 V, respectively. The role of CuPc in this device is supplying resistance. Since CuPc was also used as the collector layer of the p-type MBOT, both films can be simultaneously prepared when a monolithic device integrating resistor and MBOT is designed.

Figure 3 shows the modulation characteristics of the p-type MBOT, the output curves (I_C-V_B) and input curves (I_B-V_B) for a constant V_C. The output collector current (I_C) and

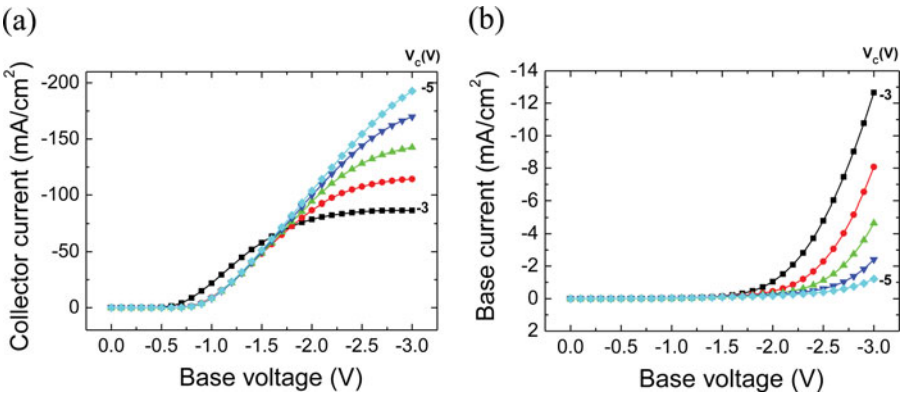

Figure 3. The modulation characteristics of the p-type MBOT under a constant collector voltage, (a) output curves (I_C-V_B) and (b) input curves (I_B-V_B).

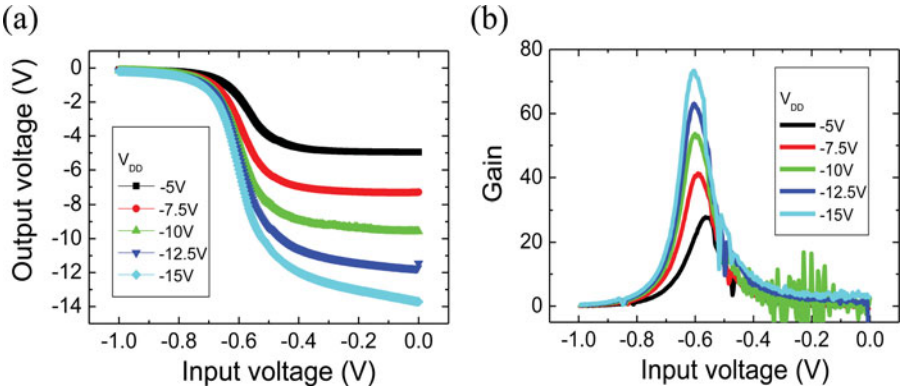

Figure 4. (a) The voltage transfer characteristics and (b) the static voltage gain of the inverter circuit for several supplied voltages.

input base current (I_B) were increased with increasing V_B. I_C increased abruptly from $V_B = -0.4$ V, and finally reached 190 mA/cm^2 at $V_B = -3$V. The on/off ratio exceeded 10^5, where on and off currents are defined as I_C at $V_B = -3$ V and $V_B = 0$ V, respectively. The magnitude of I_B was much smaller than that of I_C. This means that the I_C is amplified against the I_B. The current gain (β) was estimated to be 590 at $V_C = -5$V and $V_B = -1.7$ V.

The inverter circuit using the p-type MBOT was evaluated. Figure 4(a) shows the voltage transfer characteristics of the inverter. For the input voltage higher than −0.5 V, the output voltage was close to the power supply voltage (V_{DD}). In contrast, for the input voltage lower than −0.7 V, the output voltage drops to near 0 V. Therefore this circuit operates as an inverter. Figure 4(b) shows static voltage gain of the inverter for various V_{DD}. The maximum gain was increased for higher V_{DD}, and estimated to be 27.8, 53.6, and 73.2 at $V_{DD} = -5$ V, −10 V, and −15 V, respectively.

The resistor-transistor logic (RTL) circuit was fabricated by connecting the two resistor devices to the base electrode of MBOT in parallel (see Fig. 1). The voltage transfer characteristics of the RTL circuit are shown in Fig. 5(a). Under a constant low level (0 V) for the input B, when the input A was turned from low (0 V) to high (−3 V), then the output Y changed from high (−5 V) to low (0 V). On the other hand, under a constant high (−3 V) level for the input B, the output Y continually indicated around 0 V, whether the input A

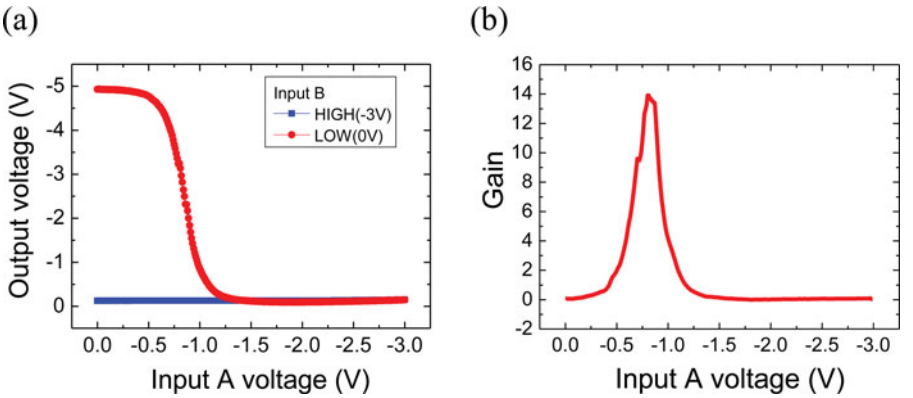

Figure 5. (a) The voltage transfer characteristics of the RTL circuit when the input B is low (red line) or high (blue line). (b) The static voltage gain of the RTL circuit at $V_{DD} = -5$ *V*.

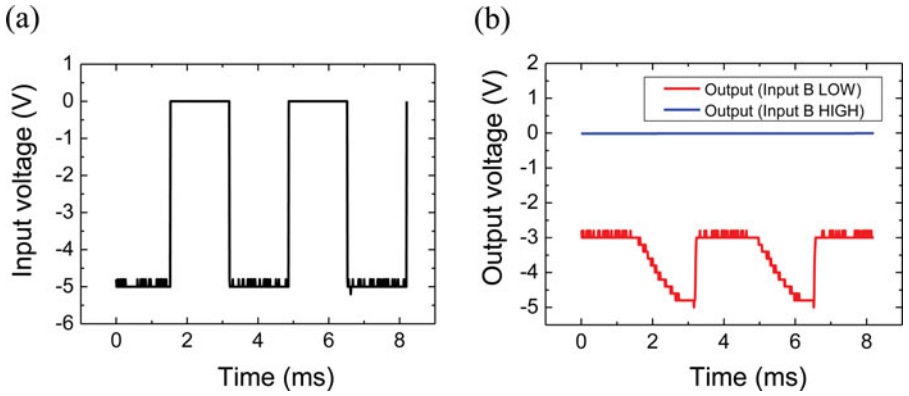

Figure 6. The transient response of the RTL circuit, (a) square-wave input signal to the input A, (b) output transient voltages when input B is low (0 *V*, red line) and high (−5 *V*, blue line).

was low or high. Thus, the output Y becomes high only when both input A and B were low, and becomes low in other case. This behavior indicates that this circuit operates as NOR gate. Figure 5(b) shows static voltage gain of the RTL circuit, which is defined as a slope in the transfer voltage curve. A maximum value was estimated to be 13.9. This high value results from the sharp transfer curve and high on/off ratio of the MBOT device in low voltage region. The voltage gain depends on the resistance of the input resistor. Higher input resistance gives smaller static voltage gain, but it is desirable to prevent an influence to front-stage circuits. Generally, when input resistance of the logic gate becomes lower, larger output current from the front-stage gate is required, causing unstability of the input signal. Therefore, the input resistance in RTL has a favorable value in the trade-off between voltage gain and circuit stability.

The dynamic characteristics of the RTL are shown in Fig. 6. The square-wave input signal was entered to the input A with amplitude of 5 V and frequency of 300 Hz. The input B was a constant voltage at high (−5 V) or low (0 V). When the input B was high, the output voltage showed no response at around 0 V. When the input B was low, the output voltage periodically changed from high (−5 V) to low (−2.8 V) according to signal wave of the input A. Thus, it was revealed that this NOR gate could operate at 300 Hz. The rising time from low to high was much faster than the falling time. This possibly indicates that charging to the base electrode of the MBOT to pull up the voltage is much faster than discharging the accumulated charges.

Conclusion

The NOR gate was fabricated by resistor-transistor logic (RTL) using the p-type MBOT and two resistor devices. The transfer curves for various combination of the two input singals demonstrated NOR behavior: when either input (A or B) was turned from low to high, the output changed from high to low. This NOR gate showed high voltage gain of 13.9 and operation frequency of 300 Hz.

Acknowledgment

This research was supported by the New Energy and Industrial Technology Development Organization (NEDO), a Grant-in-Aid for Scientific Research from the Japan Society for the Promotion of Science (JSPS).

References

[1] Sekitani, T., Zschieschang, U., Klauk, H., & Someya, T. (2010). *Nat. Mater.*, *9*, 1015.
[2] Ko, S. H., Pan, H., Grigoropoulos, C. P., Luscombe, C. K., Frechet, J. M. J., & Poulikakos, D. (2007). *Nanotechnology*, *18*, 345202.
[3] Subramanian, V., Chang, P. C., Lee, J. B., Molesa, S. E., & Volkman, S. K. (2005). *IEEE Trans. Compon. Packaging Technol.*, *28*, 742.
[4] Fukuda, K., Takeda, Y., Yoshimura, Y., Shiwaku, R., Lam Truc, T., Sekine, T., Mizukami, M., Kumaki, D., & Tokito, S. (2014). *Nature Communications*, *5*, 4147.
[5] Chen, P. C., Fu, Y., Aminirad, R., Wang, C., Zhang, J. L., Wang, K., Galatsis, K., & Zhou, C. W. (2011). *Nano Letters*, *11*, 5301.
[6] Guerin, M., Daami, A., Jacob, S., Bergeret, E., Benevent, E., Pannier, P., & Coppard, R. (2011). *IEEE Transactions on Electron Devices*, *58*, 3587.
[7] Kudo, K., Wang, D. X., Iizuka, M., Kuniyoshi, S., & Tanaka, K. (1998). *Thin Solid Films*, *331*, 51.
[8] Fujimoto, K., Hiroi, T., Kudo, K., & Nakamura, M. (2007). *Adv. Mater.*, *19*, 525.
[9] Chao, Y. C., Lai, W. J., Chen, C. Y., Meng, H. F., Zan, H. W., & Horng, S. F. (2009). *Appl. Phys. Lett.*, *95*, 203305.
[10] Ou, T. M., Cheng, S. S., Huang, C. Y., Wu, M. C., Chan, I. M., Lin, S. Y., & Chan, Y. J. (2006). *Appl. Phys. Lett.*, *89*, 183508.
[11] Cheng, S. S., Chen, J. H., Chen, G. Y., Kekuda, D., Wu, M. C., & Chu, C. W. (2009). *Org. Electron.*, *10*, 1636.
[12] Huang, J. Y., Yi, M. D., Ma, D. G., & Hummelgen, I. A. (2008). *Appl. Phys. Lett.*, *92*, 232111.
[13] Fujimoto, S., Nakayama, K., & Yokoyama, M. (2005). *Appl. Phys. Lett.*, *87*, 133503.
[14] Nakayama, K., Fujimoto, S., & Yokoyama, M. (2009). *Org. Electron.*, *10*, 543.
[15] Nakayama, K., Akiba, R., & Kido, J. (2012). *Appl. Phys. Express*, *5*, 094202.